Degradation pathways of ethyl violet by photocatalytic reaction with ZnO dispersions

Chiing-Chang Chen*

Department of General Education, National Taichung Nursing College, Taichung 403, Taiwan, ROC

Abstract

The photodegradation of ethyl violet (EV; N,N,N',N',N'',N''-hexaethyl-pararosaniline; C.I. 42600) dye was examined in aqueous ZnO dispersions under UV light irradiation. The techniques of HPLC–ESI-MS have been used to identify the various intermediates and to investigate the photocatalytic mechanism of the dye after low watt irradiation. The degradation progresses through competitive reactions such as N-de-ethylation and oxidative degradation. Twenty-six intermediates have been detected by HPLC–ESI-MS. The N-de-ethylation took place in a stepwise manner to yield mono-, di-, tri-, tetra-, penta-, and hexa-ethylated EV species while the oxidative degradation yielded 4-diethylaminophenol (DAP), 4-diethylamino-4′-diethylaminobenzophenone (DDBP) and their N-de-ethylated products, which were found for the first time in the ZnO-mediated photocatalysis process. Moreover, the hydroxyethylated intermediates formed in the N-de-ethylated EV, DDBP, and DAP processes were also separated and identified for the first time. For decolorization of dyes, the possible photodegradation pathways were proposed and discussed.
© 2006 Elsevier B.V. All rights reserved.

Keywords: Ethyl violet; N-De-ethylation; ZnO; Photocatalytic; Dyes

1. Introduction

In recent years, semiconductor-assisted photocatalysis has been extensively investigated, mainly due to its capacity to degrade a high number of recalcitrant chemicals in gaseous or aqueous systems, through relatively inexpensive procedures. TiO$_2$ is the most commonly used effective photocatalyst for a wide range of organic chemical degradation [1–4]. While most photocatalytic studies have used anatase TiO$_2$ as photocatalyst, numerous studies have been carried out to evaluate the potentiality of other metal oxides. Among others, zinc oxide appears as a very promising photocatalyst for degradation of organic solutes in aqueous systems. In some cases, ZnO has actually proven more effective than TiO$_2$ [5,6].

The ZnO-mediated photocatalysis process has been successfully used to degrade dye pollutants for the past few years [7–12]. ZnO is available at low cost, which gives it an important advantage. The initial step in ZnO-mediated photocatalysed degradation is proposed to involve the generation of an (e^-/h^+) pair leading to the formation of hydroxyl radical ($^\bullet$OH), superoxide radical anions ($O_2^{\bullet-}$), and hydroperoxyl radical ($^\bullet$OOH). These radicals are the oxidizing species in the photocatalytic oxidation processes. The high oxidative potential of the holes (h_{vb}^+) in the catalyst permits the direct oxidation of organic dye to reactive intermediates. Very reactive hydroxyl radicals can also be formed either by the decomposition of water or by the reaction of the hole with OH$^-$. The hydroxyl radical is an extremely strong, non-selective oxidant ($E^0 = +3.06$ V), which leads to the partial or complete mineralization of several organic chemicals. The dye degradation efficiency depends on the oxygen concentration, which determines the efficiency with which conduction band electrons (e_{cb}^-) are scavenged or the recombination of (e^-/h^+) is prevented. The electron in the conduction band can be picked up by the adsorbed dye molecules, leading to the formation of dye radical anion and the degradation of the dye [5].

Triphenylmethane dyes are used extensively in the textile industry for dying nylon, cotton, wool, and silk, as well as for coloring oils, fats, waxes, varnishes, and plastics. The paper, food, cosmetic, and leather industries are also major consumers of these dyes [13,14]. Thyroid peroxidase-catalyzed oxidation of the triphenylmethane dyes results in the formation of

---

various *N*-de-alkylated primary and secondary aromatic amines, which have structures similar to aromatic amine carcinogens [15].

In earlier reports [16–19], it was noted that some of the triphenylmethane dyes in the TiO$_2$-assisted photodegradation system that contain *N*-alkylamine groups appeared to photodegrade via two competitive pathways: one was *N*-de-alkylation of the chromophore skeleton, and the other was cleavage of the whole conjugated chromophore structure. The detailed mechanism behind the photodegradation of triphenylmethane dyes under the UV/TiO$_2$ or vis/TiO$_2$ process, however, remains unknown.

A ZnO-assisted photocatalytic degradation study of the EV dye under UV-365 nm light irradiation has never been reported. This research focuses on identification of the reaction intermediates and understanding the mechanistic details of the photodegradation of EV dye in the UV/ZnO process as a foundation for future applications.

2. Experimental

2.1. Materials and reagents

The ZnO nanoparticle (particle size, ca. 50–70 nm; BET area, ca. 15–25 m^2/g) was purchased from Aldrich Chemical Co. The ZnO powder was used as received as a photocatalyst without further purification. De-ionized water was used throughout this study. The water was purified with a Milli-Q water ion-exchange system (Millipore Co.) to give a resistivity of 1.8×10^7 Ω cm.

EV (with a guaranteed purity of 98%) was purchased from Tokyo Kasei Kogyo Co. and used as such without further purification. The chemical structure of EV is shown in Fig. 1. HPLC analysis confirmed the presence of EV as the only organic compound. Stock solutions containing 1 g/L of EV in water were prepared, protected from light, and stored at 4 °C. Reagent-grade ammonium acetate, nitric acid, sodium hydroxide, and HPLC-grade methanol were obtained from Merck.

2.2. Apparatus and instruments

The C-75 Chromato-Vue Cabinet of UVP provides a wide area of illumination from the 15-W 365 nm and UV tubes positioned on two sides of the cabinet interior. The following instruments were used: a Waters ZQ LC/MS system, equipped with a Waters 1525 Binary HPLC pumps, a Waters 2996 Photodiode Array Detector, a Waters 717plus Auto sampler, and a Waters micromass-ZQ4000 Detector.

2.3. Experimental procedures

An aqueous ZnO dispersion was prepared by adding ZnO powder to a 100 mL solution containing EV at appropriate concentrations. For reaction in different pH media, the initial pH of the suspensions was adjusted by addition of either NaOH or HNO$_3$ solution. Prior to irradiation, the dispersions were magnetically stirred in the dark for ca. 30 min to ensure the establishment of the adsorption–desorption equilibrium. Irradiations were carried out using two UV-365 nm lamps (15 W). At given irradiation time intervals, the dispersion was sampled (5 mL), centrifuged, and subsequently filtered through a Millipore filter (pore size, 0.22 μm) to separate the ZnO particles.

Blank experiments performed in flask without addition of ZnO show no appreciable decolorization of the irradiated solution, thus confirming the expected stability of EV dye under UV light irradiation. Addition of 0.5 g/L ZnO to solutions containing 50 mg/L of EV did not alter the stability of the dye in the dark.

2.4. Analytical methods

2.4.1. High-pressure liquid chromatography (HPLC)

After each irradiation cycle, the amount of the residual dye was determined by HPLC–PDA. The analysis of organic intermediates was accomplished by HPLC–PDA–ESI-MS after the readjustment of the chromatographic conditions in order to make the mobile phase compatible with the working conditions of the mass spectrometer. Two different kinds of solvents were prepared in this study. Solvent A was 25 mM aqueous ammonium acetate buffer (pH 6.9) while solvent B was methanol. LC was carried out on an Atlantis™ dC18 column (250 mm × 4.6 mm i.d., dp = 5 μm). The flow rate of the mobile phase was set at 1.0 mL/min. One linear gradient progressed from 95% A to 50% A in 20 min; then another linear gradient progressed from 50% A to 10% A in 20 min, and remained unchanged for 5 min; then another linear gradient progressed from 10% A to 95% A in 3 min.

2.4.2. Electro-spray-ionization mass-spectrometry (ESI-MS)

The column effluent was introduced into the ESI source of the mass spectrometer. Equipped with an ESI interface, the quadruple mass spectrometer with heated nebulizer probe at 350 °C was used with an ion source temperature of 100 °C. ESI was carried out with the vaporizer at 300 °C and nitrogen as sheath (80 psi) and auxiliary (20 psi) gas to assist with the preliminary nebulization and to initiate the ionization process. A discharge current of 5 μA was applied. Tube lens and capillary voltages were optimized for the maximum response during perfusion of EV standard.
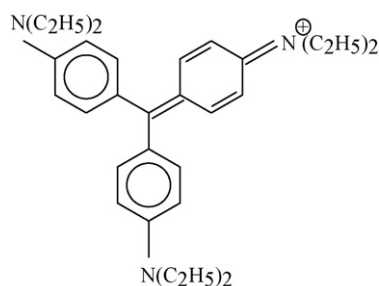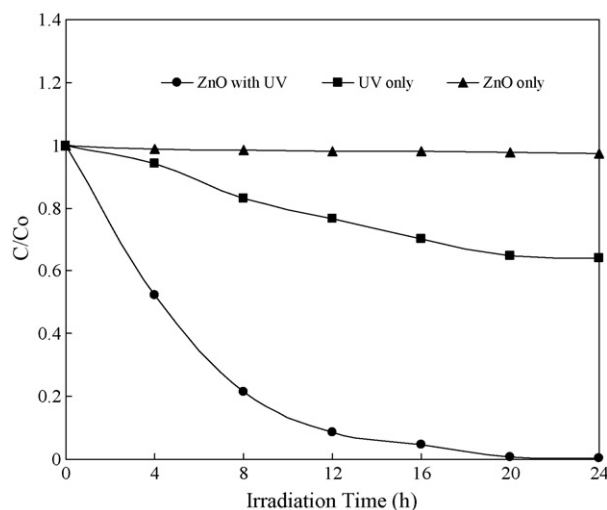

Fig. 1. Chemical structure of EV.

Fig. 2. EV degradation under the control conditions (ZnO only and UV only) and photocatalytic conditions (experimental conditions: EV = 0.05 g/L, ZnO = 0 g/L in photolysis, 0.5 g/L in photocatalysis, UV-365 nm in photolysis and photocatalysis conditions).

3. Results and discussion

3.1. Control experiments

To confirm the role of ZnO in the photocatalysis reaction, three sets of experiments were performed to compare EV degradation rates with and without catalysts. One set was performed with EV (0.05 g/L) exposed to ZnO (0.5 g/L) but no UV (the ZnO-only condition). The second set was performed by exposing EV (0.05 g/L) to UV without ZnO (the photolysis condition). Then, the third set was performed by exposing EV to ZnO (0.5 g/L) in the presence of UV irradiation (the photocatalysis condition). The results are presented in Fig. 2.

First, the experiment with ZnO only showed that the small amount of EV (about 7%) was adsorbed on the ZnO surface. Control experiments performed in the dark indicated the hydrolysis and adsorption of EV on ZnO particles did not affect its concentration during these experiments. Next, the results of the photolysis and photocatalytic experiments showed that the photolysis reaction resulted in a 19% decrease in the EV concentration after 6 h while 99.9% of EV was removed after 6 h in the case of the photocatalytic reaction. Therefore, we tentatively propose that EV photocatalytic degradation proceed by ZnO under UV illumination.

3.2. Catalyst type

Blank experiments were performed under UV irradiation without addition of any catalyst, and negligible decolorization efficiency was observed. To enhance the efficiency, TiO_2 and ZnO catalysts were examined under various process conditions. By applying the following simple first-order rate law, $-\ln(C/C_0) = kt$, to the results of the current study, a linear relationship between $-\ln(C/C_0)$ and time (t), which was consistent with first-order kinetics, was observed. The slope k of the best-fit line through the data points represents the first-order rate con-

stants for the corresponding two different catalysts. The rate constants for TiO_2 and ZnO are 0.53 and 1.01 (h^{-1}), respectively, under the same conditions; ZnO is a superior catalyst. The results showed that ZnO exhibits higher photocatalytic activity than TiO_2, and the same trend was also obtained in other studies with azo-dyes [8,20,21]. Hence, all further studies were carried out using Aldrich ZnO catalysts.

3.3. pH effect

The zero point charge for ZnO is 9.0, and above this value, the ZnO surface is predominantly negatively charged when the pH is higher than the ZnO isoelectric point. As the pH decreases, the functional groups are protonated, and the proportion of the positively charged surface increases. Thus, the electrical property of the ZnO surface varies with the pH of the dispersion [22].

The role of pH on the photodegradation was studied in the pH range of 3–10 at 50 mg/L dye concentration and 0.5 g/L catalyst loading. The pH of the solution was adjusted before irradiation and was not controlled during the course of the reaction. The photodegradation rate was found to decrease then increase with decreases in the value of pH. At higher pH values, no photocorrosion of ZnO takes place. More efficient formation of hydroxyl radical occurs in alkaline conditions. EV has a diethylamino group in its structure, which is positively charged; therefore, the dye may be absorbed onto the photocatalyst surface effectively. The formation of active •OH species is favored with higher pH values, due not only to improved transfer of holes to the adsorbed hydroxyls, but also to electrostatic abstractive effects between the negatively charged ZnO particles and the operating cationic dyes. In a good agreement with the adsorption mechanism proposed by Li et al. [17], our results indicate that the ZnO surface is negatively charged and that the EV was adsorbed onto the ZnO surface through the positive ammonium groups. Although the EV dye can be adsorbed onto the TiO_2 surface to some extent in alkaline media, the dye molecules will change to a leuco compound when the pH value is too high (pH 11).

On the other hand, a noticeable increase in the photodegradation rate of EV was observed at pH 3. In acidic solutions the photodegradation rate was higher than in neutral solutions. This is because the photodecomposition of ZnO takes place in acid and neutrals. The photocorrosion of ZnO is complete at pH lower than 4. The formation of Zn^{2+} is attributed to the oxidation of ZnO by h^+_{vb} [20,22,23]. Besides, the cationic EV dye was found difficult to adsorb onto the TiO_2 surface under acidic conditions, usually with the active •OH radicals formed in low concentrations, and hence the photodegradation process of EV remained slow. The results show that the photodegradation rate at pH 3 is higher than that at pH 9, but slower than that at pH 10.

3.4. Photocatalyst loading

The amount of photocatalyst is an important parameter that can affect the degradation rate of organic compounds in slurry photocatalytic processes. Hence, to investigate the relation between photocatalyst loading and rate constant K (h^{-1}), the amount of catalyst was varied between 0.1 and 2 g/L in a
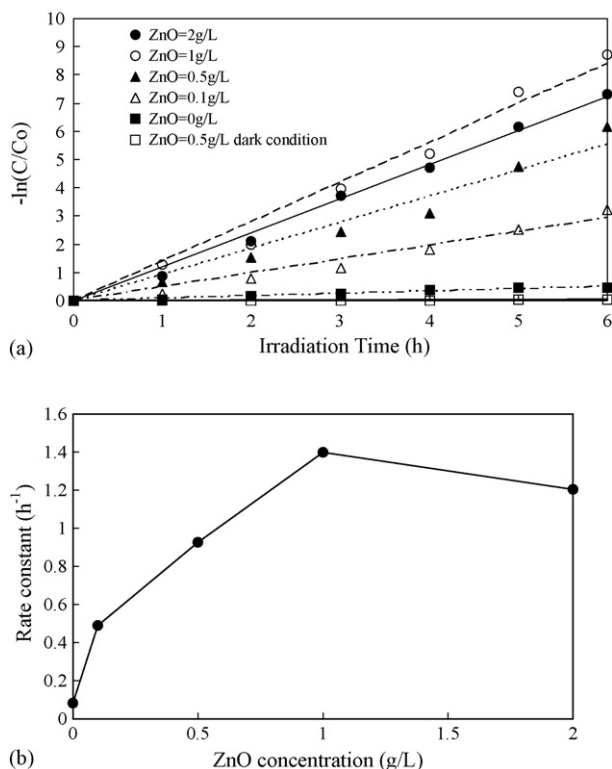
(a)

(b)

Fig. 3. Influence of the catalyst concentration on the (a) photodegradation rate (b) rate constant for the decomposition of EV. Experimental conditions: dye concentration (0.05 g/L); ZnO (2, 1, 0.5 and 0.1 g/L); pH 6; absorbance was recorded at 580 nm; continuous stirring; irradiation time, 6 h.

series of experiments under constant process conditions: dye concentration = 50 mg/L, pH 6. Fig. 3a shows first-order rate curves for various catalyst loadings. As expected, the reaction rate was found to increase then decrease with the increase in the catalyst loading (Fig. 3b). This is characteristic of heterogeneous photocatalysts, and the results are in agreement with the earlier studies [16]. The photolysis reaction resulted in a roughly 36% decrease in the EV concentration after 6 h while in the photocatalytic reaction the EV was completely decomposed after 6 h. Above 1 g/L of ZnO, the initial rate of EV degradation was not affected further by a progressive increase in the ZnO concentration. The maximal rate constant for EV appears at a ZnO concentration of around 1 g/L. This phenomenon may be due to the aggregation of ZnO particles at high concentrations causing a decrease in the number of surface active sites. Besides, aggregation of ZnO particle may also occur, when pH or ionic strength is changed. It is known, however, a practical limit of the scattering light (around 1 g/L) exists, above which the degradation rate will decrease due to the reduction of the photonic flux within the irradiated solution [9,10].

3.5. UV–vis spectra

The aqueous solution of the EV dye was slightly unstable under UV irradiation in the absence of ZnO. However, the EV dye can be degraded efficiently in aqueous EV/ZnO dispersions by UV light irradiation at 365 nm. After irradiation for 5 h, ca.

99.94% of the EV dye was degraded. During UV irradiation, the characteristic absorption band of the dye around 593.0 nm decreased rapidly with a slight hypsochromic shift (579.8 nm), but no new absorption bands appeared even in the ultraviolet range (200 nm < λ < 400 nm), indicating possible formation of a series of N-de-ethylated intermediates, cleavage of the whole conjugated chromophore structure of the EV dye, and degradation of the phenylic skeleton. Similar phenomena were also observed during the TiO$_2$-mediated photodegradation of EV [18], and crystal violet [19] under visible irradiation.

3.6. Separation of the intermediates

Temporal variations occurring in the solution of EV dye during the degradation process with UV irradiation were examined using HPLC coupled with a photodiode array detector and ESI mass spectrometry. The chromatograms at pH 6 are illustrated in Fig. 4, recorded at 580, 350, and 300 nm. With irradiation up to 6 h at pH 6, 26 components were identified, all with retention time of less than 45 min. We denoted the EV dye and its related intermediates as species A–H, A'–D', a–f, a'–c', and α–γ. Except for the initial EV dye (peak A), the other peaks initially increased before the subsequent decrease, indicating formation and transformation of the intermediates.
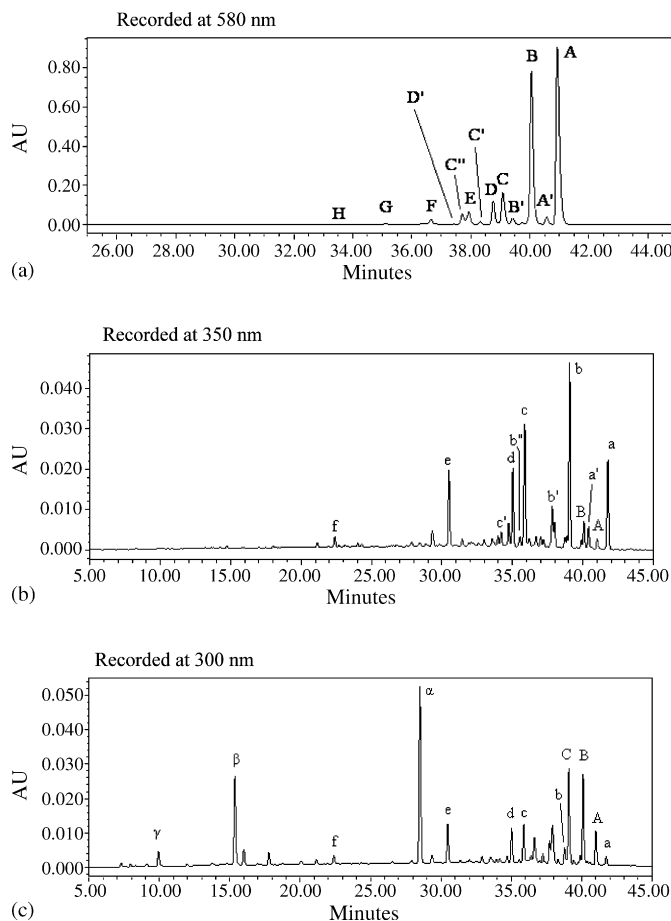

(a)

(b)

(c)

Fig. 4. HPLC chromatogram of the intermediates with ZnO 0.01 g, at pH 6, at 6 h of irradiation, recorded at: (a) 580 nm, (b) 350 nm, and (c) 300 nm.

Table 1
Identification of the *N*-de-ethylation intermediates of the EV dye by HPLC–ESI-MS

HPLC peaks	Intermediates	Abbreviation	ESI-MS peaks (m/z)	Absorption maximum (nm)
A	*N*,*N*,*N*′,*N*′,*N*″,*N*″-Hexaethylpararosaniline	EV	456.23	593.0
B	*N*,*N*-Diethyl-*N*′,*N*′-diethyl-*N*″-ethylpararosaniline	DDEPR	428.19	585.6
C	*N*,*N*-Diethyl-*N*′-ethyl-*N*′-ethylpararosaniline	DEEPR	400.16	583.6
D	*N*,*N*-Diethyl-*N*′,*N*′-diethylpararosaniline	DDPR	400.22	584.4
E	*N*-Ethyl-*N*′-ethyl-*N*″-ethyl pararosaniline	EEEPR	372.12	580.5
F	*N*,*N*-Diethyl-*N*′-ethylpararosaniline	DEPR	372.12	581.5
G	*N*-Ethyl-*N*′-ethylpararosaniline	EEPR	344.15	568.5
H	*N*,*N*-Diethylpararosaniline	DPR	344.21	570.9
A′	*N*,*N*-Diethyl-*N*′,*N*′-diethyl-*N*″-hydroxyethyl-*N*″-ethylpararosaniline	DDHEPR	472.29	617.5
B′	*N*,*N*-Diethyl-*N*′-hydroxyethyl-*N*′-ethyl-*N*″-ethylpararosaniline	DHEEPR	444.26	604.0
B″	*N*,*N*-Diethyl-*N*′,*N*′-diethyl-*N*″-hydroxyethylpararosaniline	DDHPR	444.19	597.9
C″	*N*-Hydroxyethyl-*N*-ethyl-*N*′-ethyl-*N*″-ethylpararosaniline	HEEEPR	416.16	578.3
C″	*N*,*N*-Diethyl-*N*′-ethyl-*N*″-hydroxyethylpararosaniline	DEHPR	416.28	586.9
D′	*N*,*N*-Diethyl-*N*′-hydroxyethyl-*N*′-ethylpararosaniline	DHEPR	416.22	584.4

3.7. Identification of the intermediates

3.7.1. UV–vis spectra of the intermediates

The absorption spectra of each intermediate in the visible and ultraviolet spectral region are measured corresponding to the peaks A–H, A′–D′, a–f and α–γ in Fig. 4, respectively. The *N*-de-ethylation of the EV dye has the wavelength position of its major absorption band moved toward the blue region, λ_{max}, A (EV), 593.0 nm; B, 585.6 nm; C, 583.6 nm; D, 584.4 nm; E, 580.9 nm; F, 581.5 nm; G, 568.5 nm; H, 570.9 nm. The *N*-hydroxyethylated intermediates, the *N*-de-ethylated EV species, has the wavelength position of its major absorption band moved toward the blue region, λ_{max}, A′, 617.5 nm; B′, 604.0 nm; B″, 597.9 nm; C′, 578.3 nm; C″, 586.9 nm; D′, 584.4 nm.

The oxidative degradation yields 4-diethylamino-phenol (DAP), 4-diethylamino-4′-diethylaminobenzophenone (DDBP), and their *N*-de-ethylated products. The *N*-de-ethylation of the DDBP, produced by cleavage of the EV chromophore ring structure, has the wavelength position of its major absorption band moved toward the blue region, λ_{max}, a, 380.0 nm; b, 373.1 nm; c, 365.5 nm; d, 372.1 nm; e,

357.2 nm; f, 344.2 nm. The *N*-hydroxyethylated intermediates, the *N*-de-ethylated DDBP species, has the wavelength position of its major absorption band moved toward the blue region, λ_{max}, a′, 374.7 nm, b″, 368.4 nm; b′, 369.1 nm; c″ 357.9 nm; d′, 362.1 nm. The *N*-de-ethylation of the DAP, produced by cleavage of the EV chromophore ring structure, has the wavelength position of its major absorption band moved toward the blue region, λ_{max}, α, 304.7 nm; β, 289.2 nm; γ, 279.7 nm. The data we observed above can be seen more clearly in Tables 1 and 2.

3.7.2. Mass spectra of the intermediates

The photodegraded intermediates were further identified using the HPLC–ESI mass spectrometric method. The molecular ion peaks appeared in the acid forms of the intermediates. The results of mass spectral analysis confirmed that the component A, $m/z = 456.23$, in liquid chromatogram is EV. The other components were B, $m/z = 428.19$, DDEPR; C, $m/z = 400.16$, DEEPR; D, $m/z = 400.22$, DDPR; E, $m/z = 372.37$, EEEPR; F, $m/z = 372.12$, DEPR; G, $m/z = 344.15$, EEPR; H, $m/z = 344.21$, DPR; A′, $m/z = 472.29$, DDHEPR; B′, $m/z = 444.26$, DHEEPR; B″, $m/z = 444.19$, DDHPR; C′, $m/z = 416.16$, HEEEPR; C″,

Table 2
Identification of intermediates of the destruction of the conjugated structure of the EV dye by HPLC–ESI-MS

HPLC peaks	Intermediates	Abbreviation	ESI-MS peaks (m/z)	Absorption maximum (nm)
a	4-(*N*,*N*-Diethylamino)-4′-(*N*′,*N*′-diethylamino)benzophenone	DDBP	325.18	380.0
b	4-(*N*,*N*-Diethylamino)-4′-(*N*′-ethylamino)benzophenone	DEBP	297.38	373.1
c	4-(*N*-Ethylamino)-4′-(*N*′-ethylamino)benzophenone	EEBP	269.36	365.5
d	4-(*N*,*N*-Diethylamino)-4′-aminobenzophenone	DBP	269.29	372.1
e	4-(*N*-Ethylamino)-4′-aminobenzophenone	EBP	241.20	357.2
f	4,4′-Bis-aminobenzophenone	BP	213.24	344.2
a′	4-(*N*,*N*-Diethylamino)-4′-(*N*′-hydroxyethyl-*N*′-ethylamino)benzophenone	DHEBP	341.36	374.7
b′	4-(*N*-Hydroxyethyl-*N*-ethylamino)-4′-(*N*′-ethylamino)benzophenone	HEEBP	313.34	368.4
b″	4-(*N*,*N*-Diethylamino)-4′-(*N*′-hydroxyethylamino)benzophenone	DHBP	313.40	369.1
c′	4-(*N*-Ethylamino)-4′-(*N*′-hydroxyethylamino)benzophenone	EHBP	285.37	357.9
d′	4-(*N*-Hydroxyethyl-*N*-ethylamino)-4′-aminobenzophenone	HEBP	285.31	362.1
α	4-(*N*,*N*-Diethylamino)phenol	DAP	166.21	304.7
β	4-(*N*-Ethylamino)phenol	EAP	N/A	289.2
γ	4-Aminophenol	AP	N/A	279.7

$m/z = 416.28$, DEHPR; D′, $m/z = 416.22$, DHEPR; a, DDBP; b, $m/z = 297.38$, DEBP; c, $m/z = 269.36$, EEBP; d, $m/z = 269.29$, DBP; e, EBP; f, $m/z = 213.24$, BP; a′, $m/z = 341.36$, DHEBP; b′, $m/z = 313.34$, HEEBP; b″, $m/z = 313.40$, DHBP; c′, $m/z = 285.37$, EHBP; d′, $m/z = 285.31$, HEBP; α, $m/z = 166.21$, DAP. Results of HPLC–ESI mass spectra are summarized in Tables 1 and 2.

3.7.3. Separation and identification of isomer

The absorption maximum of intermediate D (584.4 nm), F (581.5 nm), G (570.9 nm), and d (372.1 nm) occur at a longer wavelength than that of intermediate C (583.6 nm), E (580.9 nm), H (568.5 nm), and e (365.5 nm), respectively. These species correspond to the intermediates that possess from two to four (or two) ethyl groups relative to the EV (or DDBP) dye and are correlative with three (or one) pairs of isomeric molecules. One of these isomers, DEEPR, is formed by removal of an ethyl group from two different sides of the EV molecule while the other isomer in this pair, DDPR, is produced by removal of two ethyl groups from the same side of the EV structure. In the second pair of isomers, EEEPR is formed by removal of an ethyl group from each side of the EV molecule, and the other, DEPR, by removal of both two-ethyl groups from the same side of the EV structure and an ethyl group from the other side of the EV structure. In the third pair of isomers, DPR is formed by removal of two ethyl groups from two different sides of the EV molecule while EEPR is produced by removal of two ethyl groups from the same side of the EV structure and of an ethyl group from the remaining two sides of the EV structure. In the fourth pair of isomers, EEBP is formed by removal of an ethyl group from two different sides of the DDBP molecule while the other isomer in this pair, DBP, is produced by removal of two ethyl groups from the same side of the DDBP structure. Considering that the polarity of the DDPR, DEPR, DPR, and DBP species exceeds that of the DEEPR, EEEPR, EEPR, and EEBP intermediates, we expected the latter to be eluted after the former. Additionally, to the extent that two N-ethyl groups are stronger auxochromic moieties than are the N,N-diethyl or amino groups, the maximal absorption of the DDPR, DEPR, DPR, and DBP intermediates was anticipated to occur at wavelengths shorter than the band position of the DEEPR, EEEPR, EEPR, and EEBP species.

In an earlier study [24], the formation of the N-methylamino moiety by the ozone attack on the N,N-dimethylamino group is explained by the initial electrophilic attack of ozone at the nitrogen atom. From the identical intermediate, the hydroxymethylamino derivatives are also obtained. Our identical intermediates, A′–D′ (or a′–d′), are created by the N-de-ethylation of EV (or DDBP) because attack by one of the active oxygen species on the N,N-ethyl or N-ethyl group produced the hydroxyethylamino derivatives. As well, to the extent that the N-hydroxylethyl groups are weaker auxochromic moieties than are the N,N-ethyl or N-ethyl groups, the maximal absorption of the A′–D′ intermediates was anticipated to occur at wavelengths longer than the band position of the A–D species, respectively. The following results and the proposed mechanism support this argument.

3.8. Photodegradation mechanisms of EV

3.8.1. N-De-ethylation of EV

The relative distribution of all of the intermediates obtained is illustrated in Fig. 5. To minimize errors, the relative intensities were recorded at the maximum absorption wavelength for
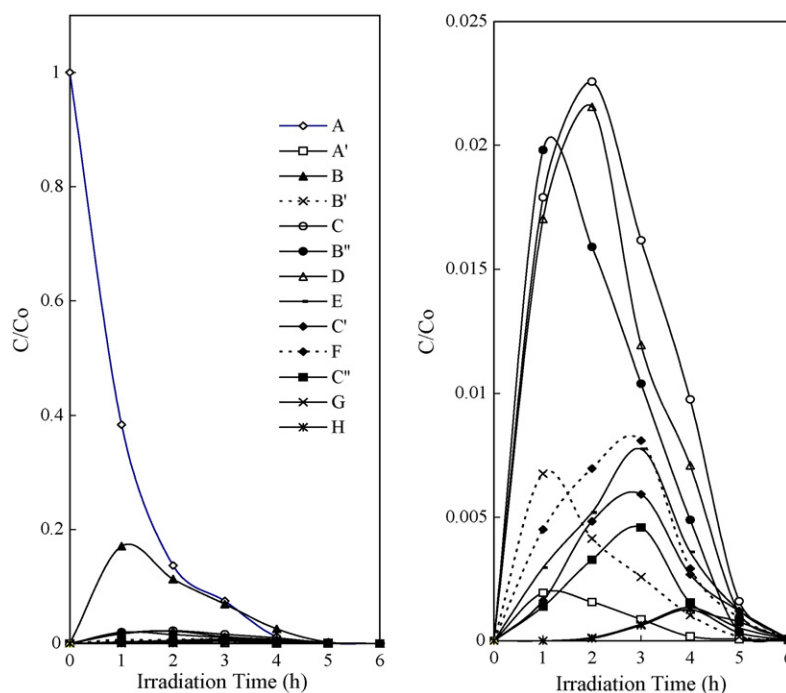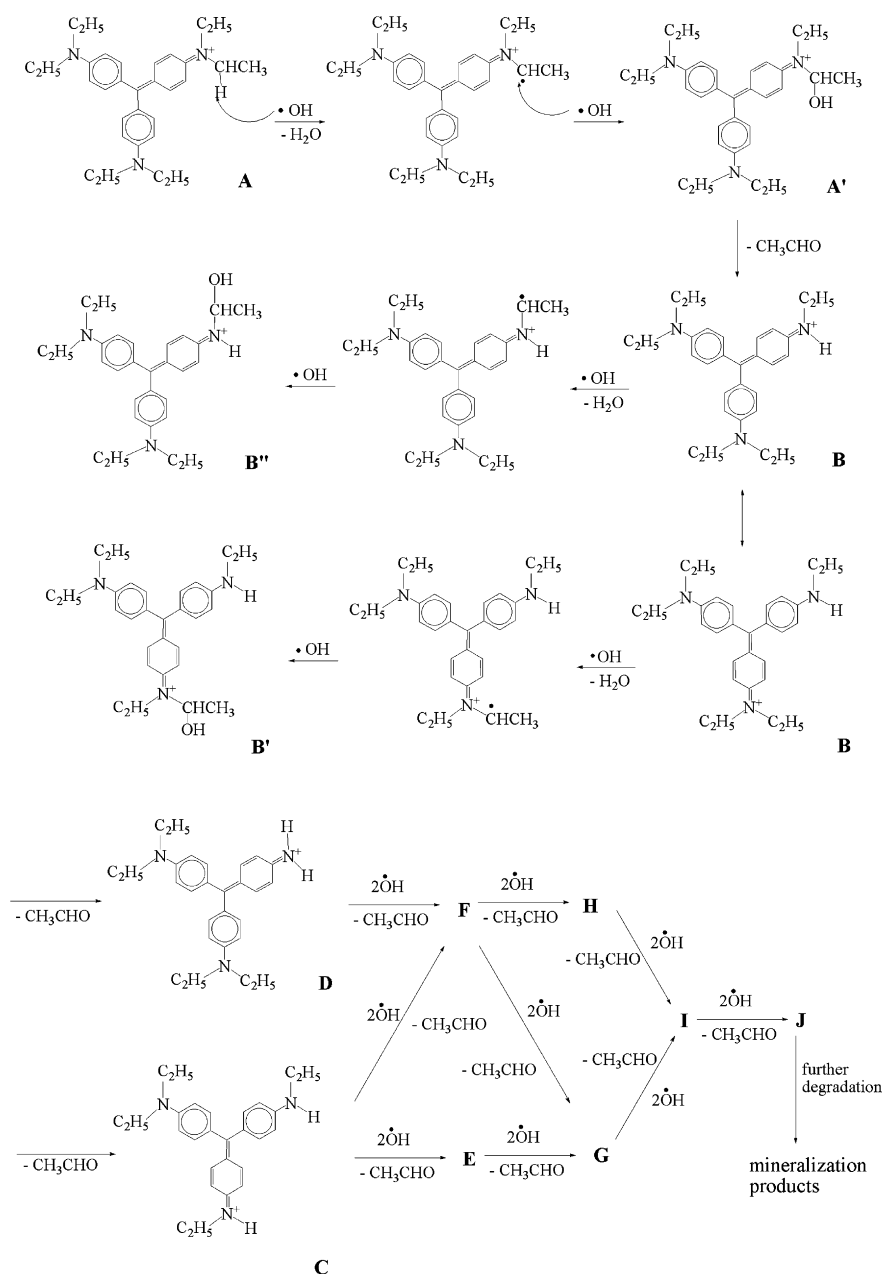

Fig. 5. Variation in the relative distribution of the N-de-ethylated products obtained from the photodegradation of the EV dye as a function of the irradiation time. Curves A–H and A′–D′ correspond to the peaks A–H and A′–D′ in Fig. 4, respectively.

each intermediate although a quantitative determination of all of the photogenerated intermediates was not achieved, owing to the lack of their appropriate molar extinction coefficients and to unavailable reference standards. The distributions of all of the *N*-de-methylated intermediates are relative to the initial concentration of EV. Nonetheless, we clearly observed the changes in the distribution of each intermediate during the photodegradation of EV. The successive appearance of the maximum of each intermediate indicates that the *N*-de-ethylation of EV, DDBP, and DAP is a stepwise photochemical process by hydroxylated intermediates.

Under UV irradiation, most of the $^\bullet$OH radicals are generated directly from the reaction between the holes and surface-adsorbed H_2O or OH^-. $O_2^{\bullet-}$ should be much less likely to be formed than $^\bullet$OH [23]. The *N*-de-ethylation of the EV dye (or DDBP) occurs mostly through attack by the $^\bullet$OH species on the *N*,*N*-diethyl portion of EV (or DDBP). Considering that the *N*,*N*-diethyl group in DDPR, DEPR, DPR, and DBP is bulkier than the *N*-ethyl group in DEEPR, EEEPR, EEPR, and EEBP molecules, $^\bullet$OH attack on the *N*-ethyl group should be favored at the expense of the *N*,*N*-diethyl group. In accord with this notion, the HPLC results showed that the DDPR, DEPR, DPR, and DBP intermediates reached maximal concentrations before the DEEPR, EEEPR, EEPR, and EEBP intermediates did.

Under basic and neutral aqueous conditions, the *N*-de-ethylation of the EV dye occurs mostly through attack by the

Scheme 1. Proposed *N*-de-ethylation pathway of the EV dye under UV irradiation in aqueous ZnO dispersions followed by the identification of several intermediates by HPLC–ESI mass spectral techniques.
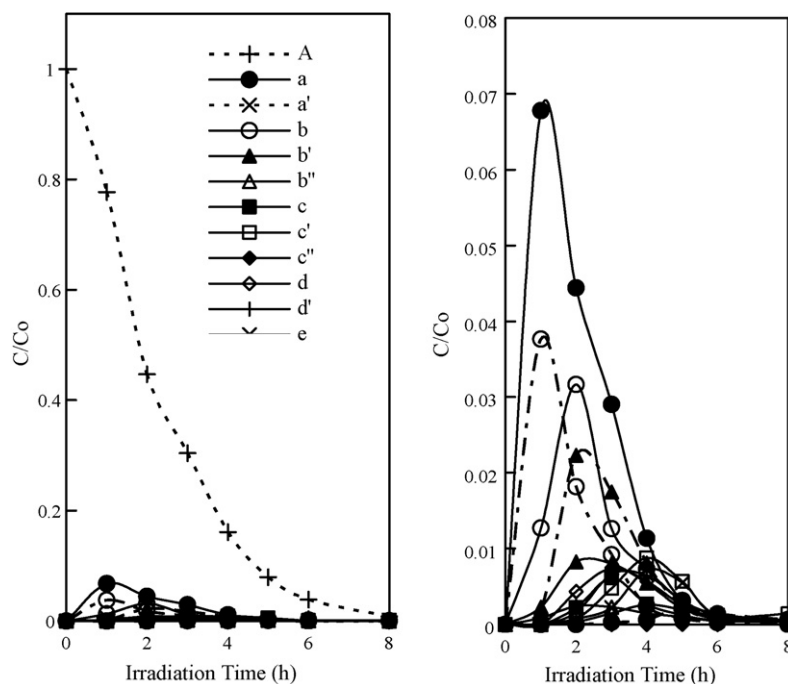
Fig. 6. Variation in the relative distribution of the destruction of the conjugated structure of products obtained from the photodegradation of the EV dye as a function of the irradiation time. Curves a–f, a′–d′, and α–γ correspond to the peaks a–f, a′–d′, and α–γ in Fig. 4, respectively.

•OH species on the N,N-diethyl group of EV. In the hydroxylation of N-hexa-ethylated intermediate (Fig. 5, curve A′), DDHEPR reached its maximum concentration after a 1 h irradiation period because of the •OH attack on the N,N-diethyl group of EV. The N-mono-de-ethylated intermediate (DDEPR) was clearly observed (Fig. 5, curve B). The other hydroxylations of N-ethylated intermediates, DHEEPR, DDHPR, HEEEPR, and DEHPR, were clearly observed (Fig. 5, curves B′–C″) to reach their maximum concentrations after 1, 1, 2, and 2-h irradiation periods, respectively. The N-di-de-ethylated intermediates DEEPR and DDPR were clearly observed (Fig. 5, curves C–D) to reach their maximum concentrations at the same time after a 2-h irradiation period because of the two competitive factors mentioned above. The other N-ethylated intermediates, DEEPR, DDPR, EEEPR, DEPR, EEPR, and DPR were clearly found (Fig. 5, curves E–H) to reach their maximum concentrations after irradiation periods of 3, 3, 4, and 4-h, respectively. The concentrations of the other de-ethylated and hydroxylated intermediates may be too low to be examined by HPLC–PDA–ESI-MS.

The successive appearance of the maximal quantity of each intermediate indicates that the N-de-ethylation of EV is a stepwise photochemical process that occurs by a dehydroxylation of N-hydroxyethylated intermediates. EV gets near the negatively charged ZnO particle surface via the positive diethylamine group. Then, before the conjugated structure is destroyed, the N-de-ethylation occurs preferentially, with the major products being N-de-ethylated EV species and their N-hydroxyethylated intermediates. The results discussed above can be seen more clearly from Scheme 1 and Table 1.

3.8.2. Oxidative degradation of EV

The oxidative degradation of the EV dye occurs mostly through attack by the •OH species on the central carbon portion of EV and produces DDBP and DAP under acidic aqueous conditions. The evolution of the concentration of the initial dye and of identified intermediates were followed as a function of irradiation time. The result is displayed in Fig. 6. The oxidative degradation intermediates DDBP and DAP were clearly observed (Fig. 6, curves a and α) to reach their maximum concentrations at the same time after a 1-h irradiation period. In the hydroxylation of DDBP (Fig. 6, curve a′), DHEBP reached its maximum concentration after a 1-h irradiation period because the •OH attacked the N,N-diethyl group of DDBP. The N-mono-de-ethylated intermediates DEBP and EAP were clearly observed (Fig. 6, curves b and β) to reach their maximum concentrations at the same time after a 2-h irradiation period. In the hydroxylation of DEBP (Fig. 6, curves b′ and b″), HEEBP and DHBP reached their maximum concentrations after a 2-h irradiation period because the •OH attacked the N,N-diethyl group of DEBP and the N-ethyl group of DEBP. The N-di-de-ethylated intermediates EEBP and AP were clearly observed (Fig. 6, curves c–d and γ) to reach their maximum concentrations after a 3-h irradiation period while DBP reached its after 4 h because the •OH attacked the N-ethyl group of DEBP and the N,N-diethyl group of DEBP. The other hydroxylations of N-ethylated intermediates, HEEBP and DEHBP, were clearly observed (Fig. 6, curves c′–d′) to reach their maximum concentrations after 3- and 4-h irradiation periods, respectively. The other N-ethylated intermediates, EBP and BP, were clearly observed (Fig. 6, curves e–f) to reach their maximum concentrations after 4- and 5-h irradiation periods, respectively. The
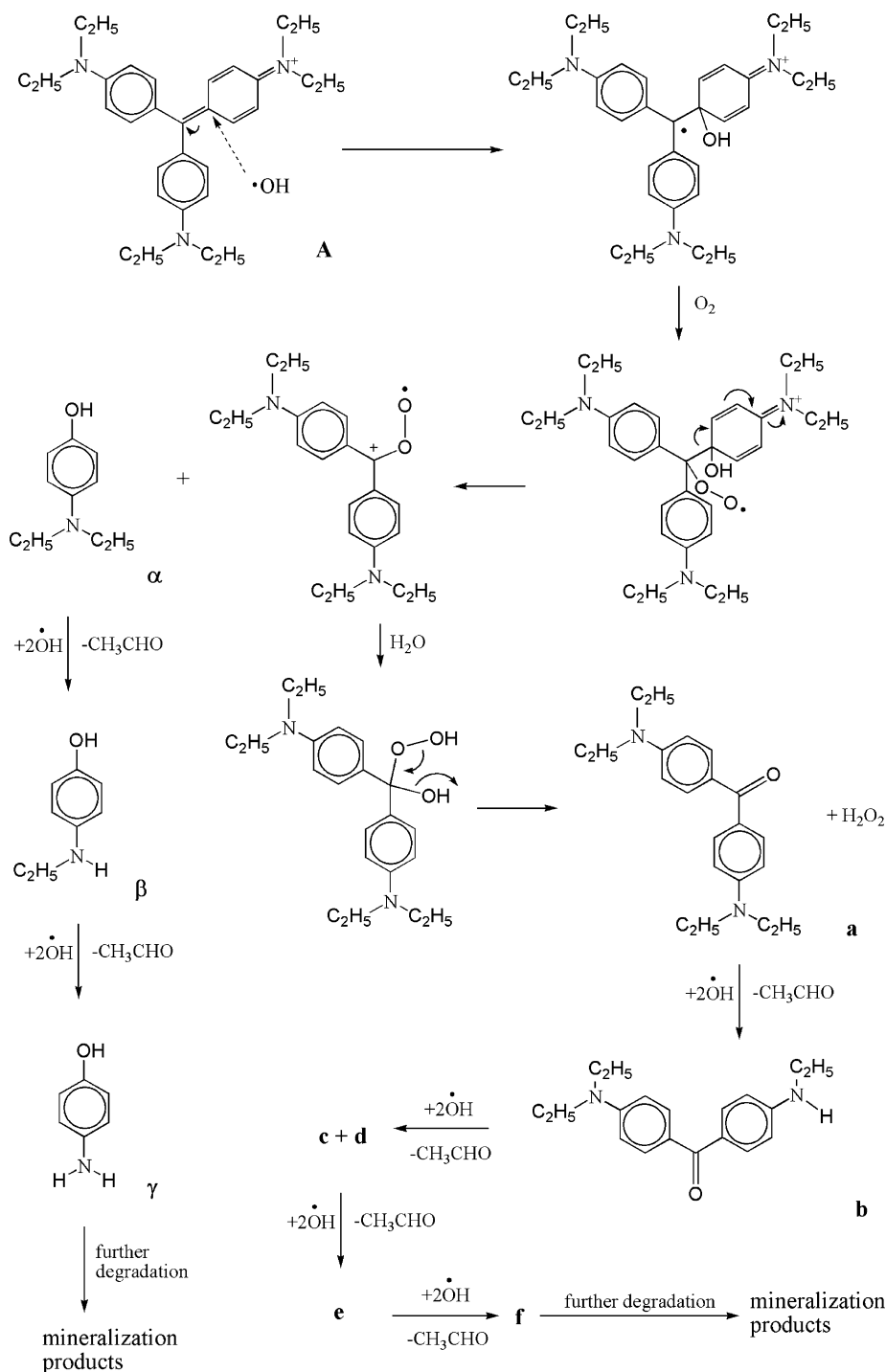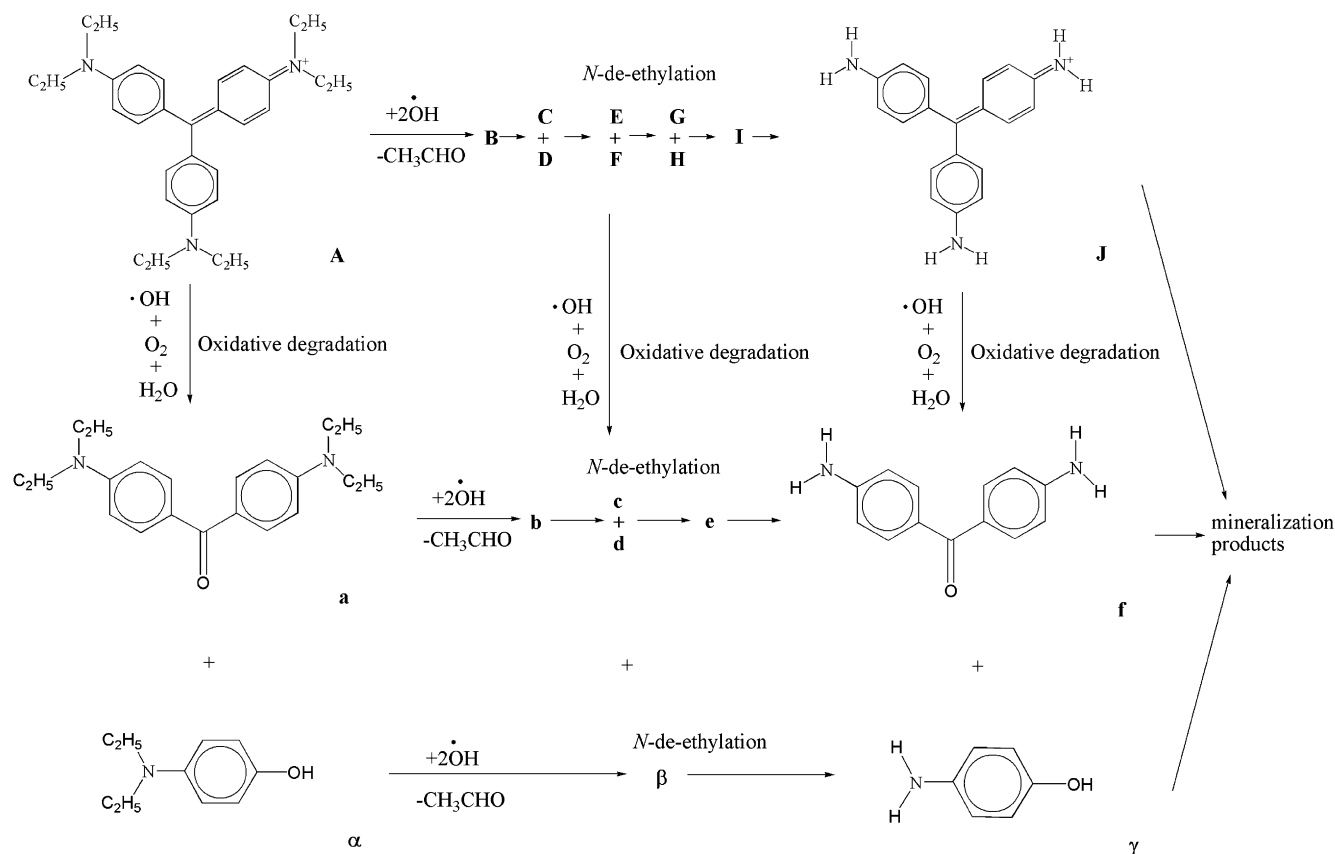
Scheme 2. Proposed pathway of the oxidative degradation of the EV dye under UV irradiation in aqueous ZnO dispersions followed by the identification of several intermediates by HPLC–ESI mass spectral techniques.

concentrations of the other hydroxylations of *N*-ethylated intermediates may be under the detectable limit.

EV is adsorbed on the positively charged ZnO particle surface via a conjugated structure. With the major photooxidation products being DDBP, DAP, their *N*-de-ethylated products, and *N*-hydroxyethylated intermediates of the de-ethylated products; the oxidative degradation (cleavage of the EV chromophore structure) predominates, and *N*-de-ethylation occurs only to a slight extent. The results we discussed above can be seen more clearly from Scheme 2 and Table 2.

According to earlier reports [25–27], most oxidative *N*-de-alkylation processes are preceded by the formation of a nitrogen-centered radical while destruction of dye chromophore structures is preceded by the generation of a carbon-centered radical [17,28,29]. Consistent with this, degradation of EV must occur via two different photooxidation pathways (destruction of

Scheme 3. Proposed photodegradation pathways of the EV dye under UV irradiation in aqueous ZnO dispersions followed by the identification of several intermediates by HPLC–ESI mass spectral techniques.

the chromophore structure and *N*-de-ethylation) due to formation of different radicals (either a carbon-centered or nitrogen-centered radical). There can be no doubt that the •OH attack on the dye yields a dye cationic radical. After this step, the cationic radical Dye•+ can undergo hydrolysis and/or use various deprotonation pathways, which in turn are determined by the different adsorption modes of EV on the ZnO particles surface.

3.8.3. Proposed photocatalytic degradation pathway of EV

On the basis of all the above experimental results, we tentatively propose the pathway of photodegradation depicted in Scheme 3. During *N*-de-ethylation, the dye molecule in the EV/ZnO system is adsorbed through the positively charged diethylamine function. Following one •OH radical attracting a hydrogen atom from the ethyl group of diethylamine, and another •OH radical attacking the diethylamine radical, forming hydroxyethylated intermediates, the subsequent hydrolysis (or deprotonation) of these intermediates yields de-hydroxyethylated intermediates, which are subsequently attacked by •OH radicals to lead ultimately to *N*-de-ethylation. The mono-de-ethylated dye DDMPR can also be adsorbed on the ZnO particle surface and implicated in other similar events (•OH radical attraction and attack, hydrolysis, or deprotonation) to yield bi-de-ethylated dye derivatives, DDPR and DMMPR.

The *N*-de-ethylation process described above continues until formation of the completely de-ethylated dye, PR.

In oxidative degradation, the dye molecule in the EV/ZnO system is adsorbed through a conjugated structure cleavage of the EV chromophore structure. Following •OH radical attack the conjugated structure yields a carbon-centered radical, which is subsequently attacked by molecular oxygen to lead ultimately to DDBP and DAP. The same process happens in the *N*-de-ethylated dye to produce the *N*-de-ethylated DDBP and DAP. The DDBP can also be adsorbed on the ZnO particle surface and be implicated in other similar events (•OH radical attraction and attack, hydrolysis or deprotonation, and/or oxygen attack) to yield a mono-*N*-de-ethylated derivative, DEBP. Moreover, the same process happens in DAP to produce EAP. The *N*-de-ethylation process described above continues until formation of the completely *N*-de-ethylated DDBP, BP, and *N*-de-ethylated DAP, AP. All of the above *N*-de-ethylation processes produce a series of *N*-de-hydroxyethylated intermediates through hydroxylation on the *N*-ethyl group. All the intermediates were further mineralized to lead to CO_3^{2-}, CO_2, and NO_3^-.

4. Conclusion

Here, we summarize the five most important findings of this report:

(1) ZnO exhibits higher photocatalytic activity than TiO_2.
(2) After a 15-W UV-365 nm irradiation for 5 h, ca. 99.94% of EV was degraded. EV could be successfully decolorized and degraded by ZnO under UV irradiation.
(3) The efficiency of EV dye photodegradation was found to first decrease then increase with a decrease in the value of pH.
(4) The photodegradation rate of the EV dye was found to increase then decrease along with an increase in the catalyst concentration. This is characteristic of heterogeneous photocatalysts.
(5) Both *N*-de-ethylation and oxidative degradation of EV take place in the presence of ZnO particles. Under basic aqueous conditions, before the conjugated structure is destroyed, *N*-de-ethylation occurs preferentially, with the major products being *N*-de-ethylated EV species and their *N*-hydroxyethylated intermediates. Under acidic aqueous conditions, the oxidative degradation (cleavage of the EV chromophore structure) predominates, and *N*-de-ethylation occurs only to a slight extent.

References

[1] A.L. Linsebigler, G.Q. Lu, J.T. Yates, Chem. Rev. 95 (1995) 735.
[2] M.A. Fox, M.T. Dulay, Chem. Rev. 93 (1993) 341.
[3] A. Hagfeldt, M. Gratzel, Chem. Rev. 95 (1995) 49.
[4] M.R. Hoffman, S.T. Martin, W. Choi, W. Bahnemann, Chem. Rev. 95 (1995) 69.
[5] H. Lachheb, E. Puazenat, A. Houas, M. Ksibi, E. Elaloui, C. Guillard, J.M. Herrman, Appl. Catal. B: Environ. 39 (2002) 75.
[6] V. Kandavelu, H. Kastien, K.R. Thampi, Appl. Catal. B: Environ. 48 (2004) 101–111.
[7] A. Akyol, H.C. Yatmaz, M. Bayramoblu, Appl. Catal. B: Environ. 39 (2002) 75.
[8] C.G. Silva, J.L. Faria, J. Photochem. Photobiol. A: Chem. 155 (2003) 133.
[9] D. Yu, R. Cai, Z. Liu, Spectrochem. Acta A 60 (2004) 1617–1624.
[10] A. Akyol, M. Bayramoglu, J. Hazard. Mater. B 124 (2005) 241–246.
[11] M.J. Height, S.E. Pratsinis, O. Mekasuwandumrong, P. Praserthdam, Appl. Catal. B: Environ. 63 (2006) 305–312.
[12] K. Mehrotra, G.S. Yablonsky, A.K. Ray, Ind. Eng. Chem. Res. 42 (2003) 2273.
[13] D.F. Duxbury, Chem. Rev. 93 (1993) 381.
[14] Ullmann's Encyclopedia of Industrial Chemistry. Part A27. Triarylmethane and Diarylmethane Dyes, 6th ed., Wiley–VCH, New York, 2001.
[15] B.P. Cho, T. Yang, L.R. Blankenship, J.D. Moody, M. Churchwell, F.A. Bebland, S.J. Culp, Chem. Res. Toxicol. 16 (2003) 285.
[16] S. Parra, S.E. Stanca, I. Guasaquillo, K.R. Thampi, Appl. Catal. B: Environ. 51 (2004) 107.
[17] X. Li, G. Liu, J. Zhao, New J. Chem. 23 (1999) 1193.
[18] C.C. Chen, C.S. Lu, Y.C. Chung, J. Photochem. Photobiol. A: Chem. 181 (2006) 120.
[19] C.C. Chen, H.J. Fan, C.S. Lu, C.Y. Jang, J.L. Jan, H.D. Lin, J. Photochem. Photobiol. A: Chem. 184 (2006) 147.
[20] A.A. Khodja, T. Sehili, J.F. Pihichowski, P. Boule, J. Photochem. Photobiol. A 141 (2001) 231.
[21] C.H. Wu, Chemosphere 57 (2004) 601–608.
[22] N. Daneshvar, D. Salari, A.R. Khataee, J. Photochem. Photobiol. A 162 (2004) 317–322.
[23] J. Fernandez, M. Kiwi, C. Lizama, J. Freer, J. Baeza, H.D. Mansilla, J. Photochem. Photobiol. A 151 (2002) 213.
[24] G.H. Kerr, O. Meth-Cohn, J. Chem. Soc. (C) (1971) 1369.
[25] G. Galliani, B. Rindone, C. Scolastico, Tetrahedron Lett. (1975) 1285.
[26] F.C. Shaefer, W.D. Zimmermann, J. Org. Chem. 35 (1970) 2165.
[27] B.L. Laube, M.R. Asirvatham, C.K. Mann, J. Org. Chem. 42 (1977) 670.
[28] J. Zhao, T. Wu, K. Wu, K. Oikawa, H. Hidaka, N. Serpone, Environ. Sci. Technol. 32 (1998) 2394.
[29] G. Liu, X. Li, J. Zhao, H. Hidaka, N. Serpone, Environ. Sci. Technol. 34 (2000) 3982.